

High loading and monodispersed Pt nanoparticles on multiwalled carbon nanotubes for high performance proton exchange membrane fuel cells

Madhu Sudan Saha, Ruying Li, Xueliang Sun*

Department of Mechanical and Materials Engineering, The University of Western Ontario, London, Ontario N6A 5B9, Canada

Received 28 September 2007; received in revised form 9 November 2007; accepted 12 November 2007

Available online 21 November 2007

Abstract

Composite electrodes consisting of Pt nanoparticles-supported on multiwalled carbon nanotubes grown directly on carbon paper (Pt/CNTs/carbon paper) have been synthesized by a new method using glacial acetic acid as a reducing agent. Transmission electron microscopy (TEM) images show that the Pt nanoparticles with high density and relative small in size (2–4 nm) were monodispersed on the surface of CNTs. X-ray photoelectron spectroscopy (XPS) analysis indicates that the glacial acetic acid acts as a reducing agent and has the capability of producing a high density of oxygen-containing functional groups on the surface of CNTs that leads to high density and monodispersion of Pt nanoparticles. Compared with standard Pt/C electrode, the Pt/CNT/carbon paper composite electrodes exhibit higher electrocatalytic activity for methanol oxidation reaction and higher single-cell performance in a H₂/O₂ fuel cell.

© 2007 Elsevier B.V. All rights reserved.

Keywords: High loading; Pt nanoparticles; Carbon nanotubes; Glacial acetic acid; Electrocatalysis; Proton exchange membrane fuel cells

1. Introduction

Proton exchange membrane fuel cells (PEMFCs) have generated strong interest as sources of “green” power for automobiles and portable electronics due to their compact design and high-power density at lower temperatures (55–95 °C) [1,2]. It is well known that the activity of a catalyst depends significantly on the size of the Pt particles and their dispersion pattern over the support structures [3]. It has been found that the optimal dispersion pattern and Pt particle size can be obtained by using an appropriate preparative procedure on an ideal supporting material [4]. The ideal support should have the following structure and properties: (i) high-surface area and good electronic property, (ii) good reactant gas access to the electrocatalysts, and (iii) high-electrochemical stability under fuel cell operating conditions [5,6]. Usually, carbon black-supported Pt electrocatalysts is used as the electrode catalyst of PEMFCs [7]. In spite of the high-surface area of the carbon black particles, the carbon black-based electrocatalyst supports have two main problems: (i) due to its dense structure, the carbon black-based support has signifi-

cant mass transfer limitations, leading to a very low-Pt utilization [5]; (ii) carbon black is known to undergo electrochemical oxidation to surface oxides and, finally, to CO₂ at the cathode in the fuel cell, where it is subjected to low pH, high potential, high humidity, and high temperatures (~80 °C). As carbon black corrodes, noble metal nanoparticles (e.g., Pt) on carbon black will detach from the electrode and possibly aggregate to larger particles, resulting in Pt surface area loss, which subsequently lowers the performance of PEMFCs [8–10]. Therefore, many efforts have been made to search for new catalyst supports [11].

In recent years, the use of carbon nanotubes (CNTs) as catalyst supports for PEMFCs and direct methanol fuel cells (DMFCs) has sparked a lot of interest owing to their unique structure and properties such as high-surface area, good electronic conductivity, strong mechanical properties and high-chemical stability [12–14]. Several research groups have reported that CNT-based electrodes can increase the catalyst utilization and increase performance of PEMFCs [15–22] and DMFCs [23–26] compared to those using commercial carbon black as support. Furthermore, CNT-based electrodes have been reported to be more stable [27,28]. However, the challenge of obtaining highly dispersed Pt nanoparticles with controllable loadings on CNTs (mostly caused by the inertness of the CNT surfaces) still exists [29].

* Corresponding author. Tel.: +1 519 661 2111x87759; fax: +1 519 661 3020.
E-mail address: xsun@eng.uwo.ca (X. Sun).

One strategy to resolve this issue is to modify the surface of CNTs before depositing the Pt nanoparticles. Various methods including oxidation in strong acids such as HNO₃ or a H₂SO₄–HNO₃ mixture [18,23,30], sonochemical [31] and electrochemical [32,33] have been used. Another strategy is to develop various deposition methods to control the size and distribution of Pt nanoparticles on CNTs. Lee et al. [29] reviewed the recent developments in synthesis of the Pt electrocatalyst supported on CNTs for PEMFC applications. Many approaches for deposition of Pt nanoparticles on CNTs have been developed. These include impregnation [23,34,35], electroless plating [15], ion-exchange [36], electrodeposition [37–40], and sputter deposition [41,42]. Nevertheless, in comparison with the carbon-supported catalysts, highly dispersed with high loading of Pt nanoparticles supported on the CNTs have not been achieved. Liu et al. [15] synthesized high-Pt loading on functionalized CNTs by an electroless plating procedure. However, the Pt nanoparticles aggregate as relatively large particles (1–5 nm) rather than uniformly dispersing on CNTs [15]. Villers et al. [22] prepared Pt nanoparticles supported on CNTs grown on carbon paper with a loading of 0.44 mg_{Pt} cm⁻² and Wang et al. [43] obtained higher metal loading of 15.4 wt.% on CNTs. However, both of these use multiple steps and repetitive processes. Thus, the synthesis of highly dispersed Pt catalysts with high-PEMFC cathode loading values till remains a challenge.

In this paper, we demonstrate a new synthetic method for preparing uniformly dispersed high-loading Pt nanoparticles on CNTs grown directly on carbon paper. The CNT-supported Pt catalysts were synthesized by the reduction of Pt precursor with glacial acetic acid. The resultant composite electrodes of Pt/CNT/carbon paper were characterized by SEM, XPS and TEM. The catalytic performance was evaluated by fuel cell station.

2. Experimental

2.1. Growth of CNTs on carbon paper

The CNTs were synthesized in the CVD reactor by decomposing a hydrocarbon gas on catalytic Co–Ni particles deposited on the fibers of carbon paper. This has been described in detail elsewhere [44]. In the reactor, a small piece of carbon paper (E-TEK Division, PEMEAS Fuel Cell Technologies, Somerset, NJ) was loaded with the catalyst. The carbon paper was then fixed across the section of the inner quartz tube and connected to the two electrodes. All gases fed into the inner quartz tube were forced to go through a 2.5 cm × 2.5 cm section of the carbon paper before exiting the reactor. Under the applied potential, the carbon paper was heated within seconds by the Joule effect up to a temperature high enough to decompose the gas used to grow nanotubes. Prior to Co–Ni deposition, the carbon paper was pretreated with methanol for 30 min, in order to improve the homogeneity of the Co–Ni particle sizes and their distribution on the carbon paper. The growth of CNTs was then carried out at 800 °C for 10 min in 90% Ar, 5% H₂, and 5% C₂H₄. Finally, the system was cooled under an Ar atmosphere. In the following

discussion, the CNTs grown on carbon paper were denoted as CNTs/carbon paper.

2.2. Preparation of Pt nanoparticles on CNTs/carbon paper

Before deposition of Pt nanoparticles, the CNTs/carbon paper was oxidized chemically in 5.0 M HNO₃ aqueous solution for 5 h. Afterward, it was washed thoroughly with deionized water until the pH of the rinsing water became neutral, and then dried under vacuum at 90 °C for 5 h. Platinum acetylacetonate, Pt(acac)₂, was used as a precursor salt and was purchased from Aldrich. Glacial acetic acid (99.8%) obtained from Fluka was used as received without further purification. CNTs/carbon paper-supported Pt electrocatalysts were prepared by reduction of Pt precursors with glacial acetic acid. A typical preparation procedure consists of the following steps: in a 50 mL beaker, the required amount of Pt(acac)₂ was added into 25 mL of glacial acetic acid and it was agitated in an ultrasonic bath for 10 min at room temperature. Then the CNTs/carbon paper was added to the solution and sonicated for 2 min. The beaker was placed on a hot plate and heated at a temperature of 110 ± 2 °C for about 5 h with constant stirring. Afterward, the Pt nanoparticles-supported CNTs/carbon paper (Pt/CNTs/carbon paper) composites were washed with deionized water and dried at 90 °C over night in a vacuum oven. The reproducibility of the electrocatalytic activity of Pt/CNTs/carbon paper was tested using three identical samples prepared in the same manner. The Pt loading in the Pt/CNT/carbon paper composites was determined by inductively coupled plasma-optical emission spectroscopy (ICP-OES).

2.3. Morphological and structural characterization

The morphologies of the CNTs/carbon paper before and after Pt nanoparticle deposition were examined using an X-ray photoelectron spectroscopy (XPS) (Kratos Analytical, UK), scanning electron microscope (SEM) (Hitachi S-2600 N), and transmission electron microscopy (TEM) (Philips CM10).

2.4. Electrochemical measurements

The electrochemical measurements were carried out by using an Autolab potentiostat/galvanostat (Model, PGSTAT-30, Ecochemie, Brinkman Instruments) in a three electrode, two-compartment configuration cell. A Pt wire served as the counter electrode and a saturated calomel electrode (SCE) was used as the reference electrode. All potentials in this paper are quoted against SCE. Purified Ar (99.9998%) and O₂ (<99.5%) gases were purchased from Praxair Canada Inc.

For comparison purposes, a conventional electrode made with commercially available 30 wt.% Pt/C obtained from E-TEK was also evaluated. This electrode was prepared with a procedure similar to the one described by Gojkovic et al. [45]. A 5-mg catalyst was sonically mixed with 1 mL 5 wt.% Nafion[®] solution (Ion Power Inc., USA) to make a suspension. The catalyst films were prepared by dispersing 5 μL of the resultant suspension on a glassy carbon (GC, diameter: 3 mm) electrode to achieve a

total Pt loading of 0.1 mg cm^{-2} on the GC electrode. The catalyst films were dried in air at room temperature.

For the measurement of hydrogen electrosorption curves, the potential was cycled between -0.25 and $+1.2 \text{ V}$ at 50 mV s^{-1} to obtain the voltammograms of hydrogen adsorption in Ar-purged $0.5 \text{ M H}_2\text{SO}_4$ aqueous solution. For cyclic voltammetry (CV) of methanol oxidation, the electrolyte solution was $2 \text{ M CH}_3\text{OH}$ in $1 \text{ M H}_2\text{SO}_4$ aqueous solution. All experiments were carried out at room temperature (25°C).

2.5. Preparation and characterization of membrane electrode assembly (MEA)

A gas diffusion layer was applied on one side of the Pt/CNT/carbon paper composite. The gas diffusion ink was prepared by ultrasonating the required quantity of carbon black (Vulcan XC-72, Cabot) and polytetrafluoroethylene (PTFE) solution in a mixture of isopropanol and deionized water (80:20 volume ratio) for 30 min followed by a magnetic stirring for about 1 h [46]. The carbon loading was approximately 3.5 mg cm^{-2} and PTFE content was 30 wt.%. The gas diffusion layer was sintered at 350°C in Ar for 1 h.

To fabricate MEAs, the cathode was CNT/carbon paper composite with Pt loading of 0.42 mg cm^{-2} while the standard E-TEK gas diffusion electrode (30 wt.% Pt/C, $0.5 \text{ mg}_{\text{Pt}} \text{ cm}^{-2}$) was used as the anode electrode. For comparison, another MEA was made using two standard E-TEK gas diffusion electrodes ($0.5 \text{ mg}_{\text{Pt}} \text{ cm}^{-2}$) as anode and cathode. The electrode area was 1.0 cm^2 and typical loading of Nafion ionomer in all electrodes was in the range of $0.9\text{--}1.0 \text{ mg cm}^{-2}$. Nafion 112 (DuPont Inc., USA) was used as the polymer electrolyte membrane. Prior to MEA fabrication, the membrane was cleaned by immersing it in boiling 3% H_2O_2 for 1 h followed by boiling in $\text{M H}_2\text{SO}_4$ for the same duration with subsequent rinsing in boiling deionized water (1 h). This procedure was repeated at least twice to ensure complete removal of H_2SO_4 . The MEA was fabricated in-house via hot pressing at 130°C and 100 psi for 2 min. Polarization curves were measured by a single fuel cell test station (Fuel Cell Technologies Inc., USA). All MEAs were conditioned prior to testing using a series of steps. The initial stage is associated with a so-called break-in process in which the cell temperature is slowly raised (approximately 20°C h^{-1}) from ambient temperature to the operational (80°C) under N_2 . After keeping the cell under these conditions for approximately 5 h in order to allow proper conditioning of the MEA assembly, the pressure was slowly increased to the desired value. The gases were then switched to saturated H_2/O_2 , and the cell was allowed to equilibrate for a couple of hours.

3. Results and discussion

3.1. Physicochemical characterization

Fig. 1 shows the SEM and TEM images of the CNTs directly grown on the fibers of carbon paper. The carbon paper consists of carbon fibers crossing each other with diameters of $5\text{--}10 \mu\text{m}$

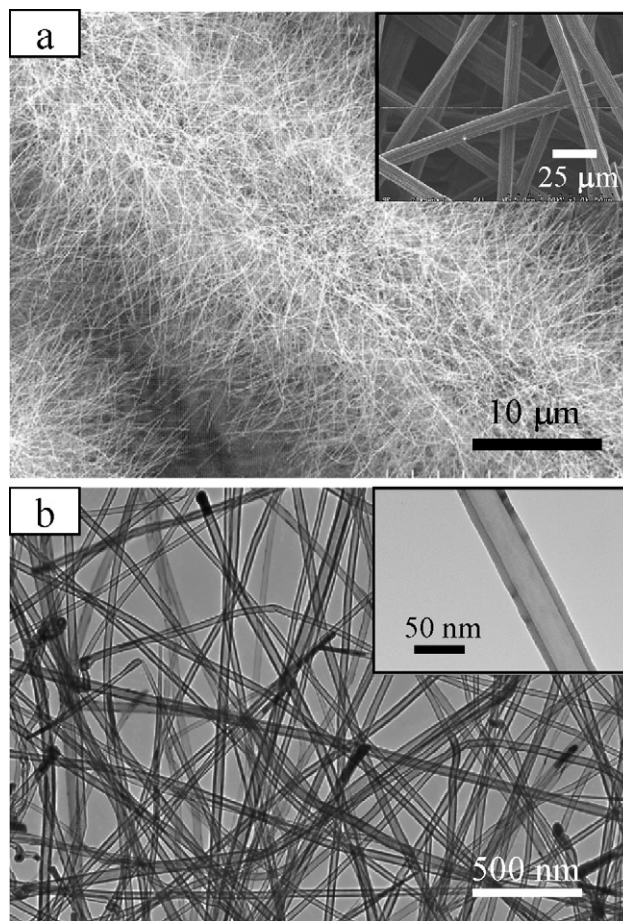


Fig. 1. (a) SEM images of CNTs grown on carbon paper (inset: carbon paper). (b) TEM images of CNTs grown on carbon paper (inset: single CNT).

(inset in Fig. 1a). As shown in Fig. 1(a), high density CNTs of $15 \mu\text{m}$ in length completely cover the surface of the carbon fibers. Further, TEM images show that the tubes are straight and clean. The diameter of the majority of the tubes ranges from 30 to 60 nm with a typical tube diameter of 50 nm shown in Fig. 1(b) inset.

Fig. 2(a–c) shows typical TEM images of CNTs/carbon paper after deposition of Pt nanoparticles synthesized by using different concentrations of Pt precursor and chemical reduction with glacial acetic acid. The right panel (a'–c') shows increased magnification TEM images of the Pt nanoparticles deposited on single CNT. The concentrations of Pt precursor are 1, 2 and 4 mM, resulting in corresponding Pt loadings of 0.11, 0.24 and 0.42 mg cm^{-2} on CNTs. It can be seen from the images that the Pt nanoparticles are highly dispersed over the entire surface of the CNTs/carbon paper. The density of Pt particles increases with the increase of the concentration of Pt precursors. The average size of the Pt nanoparticles on CNTs was also obtained by measuring 150 randomly chosen particles in the magnified TEM images. The size distribution of Pt nanoparticles is shown in the histograms in Fig. 3. It is clearly seen that the Pt nanoparticles with narrow particle size distribution have the mean nanoparticle sizes of 1.96, 2.41 and 3.65 nm, respectively, which correspond to the Pt loadings of 0.11, 0.24 and 0.42 mg cm^{-2} .

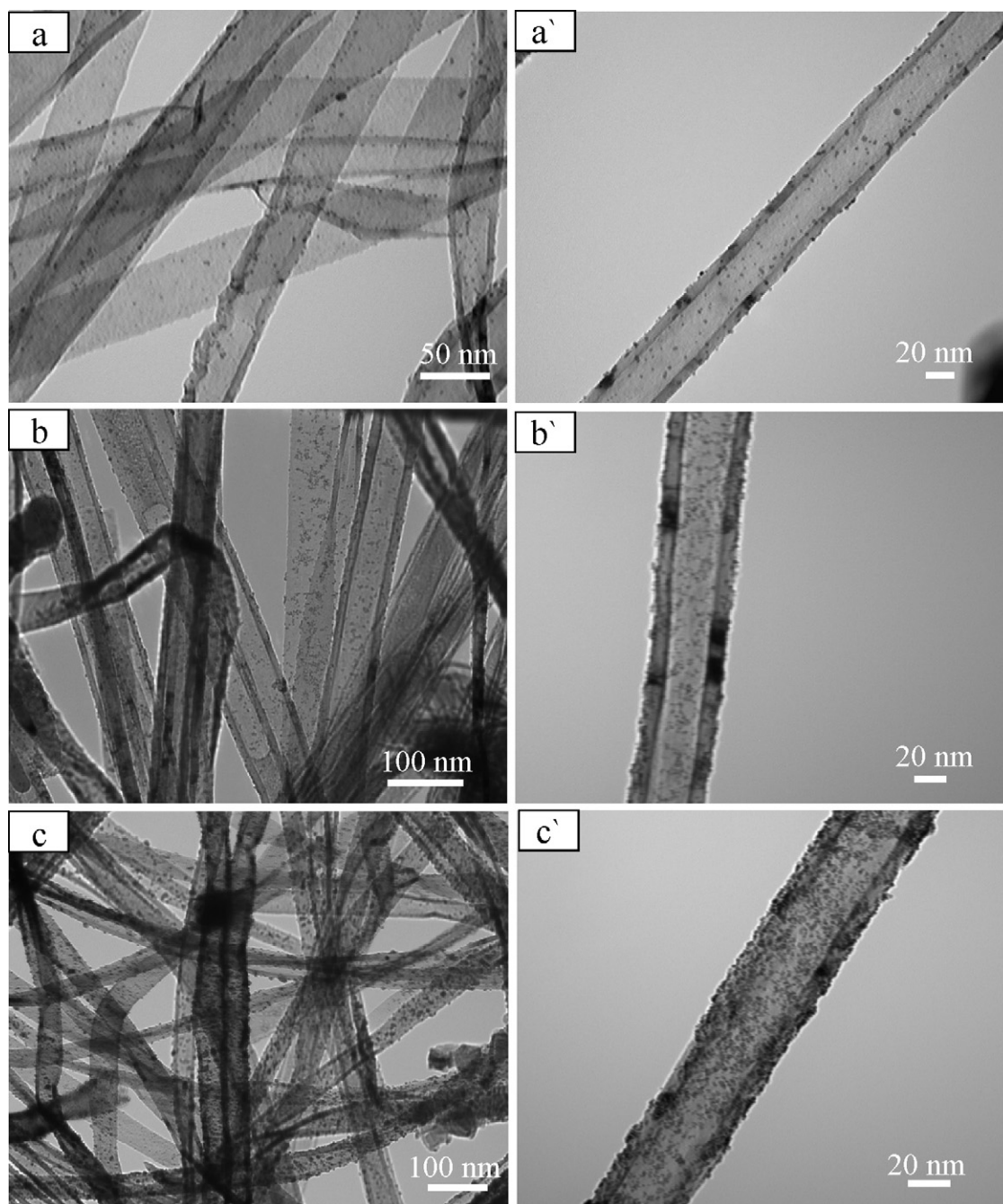


Fig. 2. TEM images of Pt nanoparticles deposited on the CNTs/carbon paper from different concentrations of Pt precursor (a) 1 mM, (b) 2 mM and (c) 4 mM in glacial acetic acid. Right panel: Pt nanoparticles deposited on single CNT. The corresponding Pt loadings on the CNTs are 0.11, 0.24 and 0.42 $\text{mg}_\text{Pt} \text{cm}^{-2}$.

Further, Pt nanoparticles supported on CNTs/carbon paper with Pt loading of 0.51 mg cm^{-2} can be obtained with a continuous Pt nanoparticle adlayer (not shown). Compared with previous attempts mentioned in the introduction, our current method based on the reduction by glacial acetic acid allows us to prepare highly dispersed Pt nanoparticles with high-Pt metal loading on CNTs.

In order to understand the Pt deposition process, XPS analyses were carried out on two samples of CNTs treated by glacial acetic acid [47]. These results strongly indicate that the glacial acetic acid under the same experimental conditions before and after deposition of the Pt nanoparticles (Fig. 4). For comparison,

the raw CNTs were also examined by XPS. A small amount of oxygen was detected on pristine CNTs due to adsorbed oxygen species (Fig. 4a), which is consistent with the results of Yu et al. [36]. In the glacial acetic acid treated CNTs, XPS spectrum (Fig. 4b) clearly shows the presence of enhanced O 1s peaks. Moreover, additional surface functional groups with the binding energy at 531.69 (48% carbonyl) and 533.31 eV (52% carboxyl) were observed after treated with glacial acetic acid itself has a strong capability of producing a high density of oxygen-containing functional groups on the surface of CNTs,

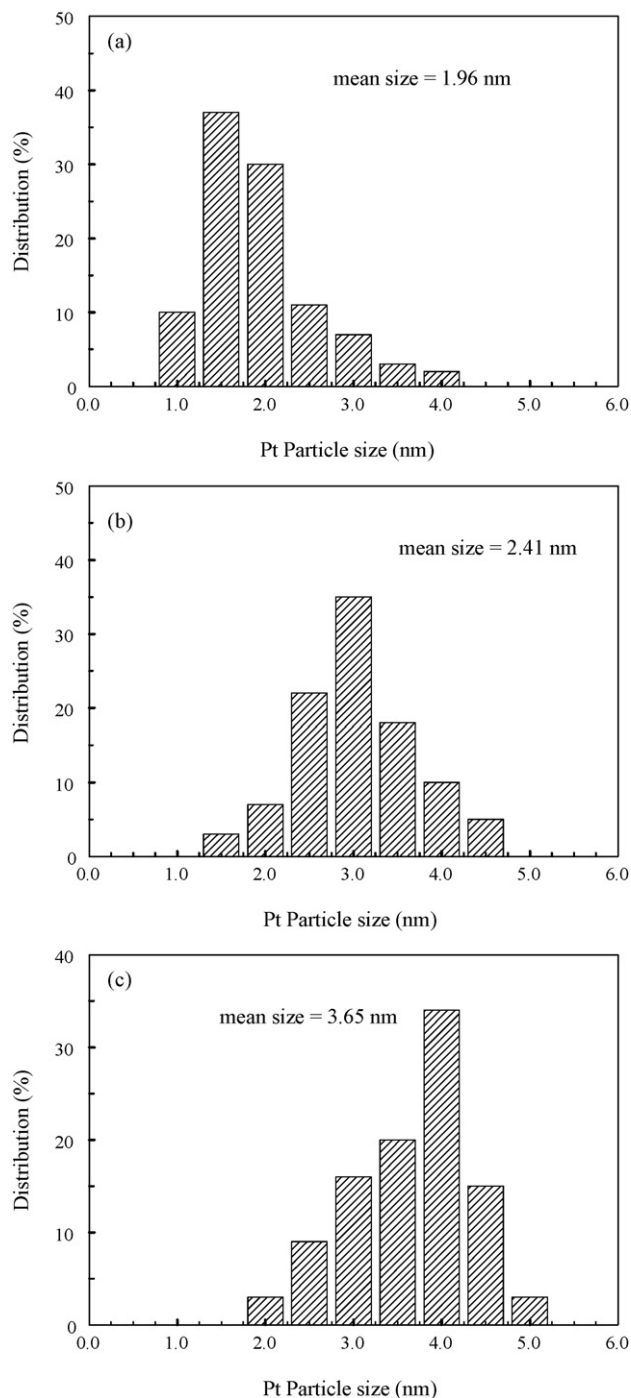


Fig. 3. Size distribution of Pt particles for the Pt/CNT/carbon paper composite electrodes prepared from different concentrations of Pt precursor (a) 1 mM, (b) 2 mM and (c) 4 mM in glacial acetic acid.

which leads to a well dispersion of Pt particles on the surface of CNTs with controlled Pt loading. For Pt nanoparticles-supported CNTs, XPS spectrum in Fig. 4(c) reveals two Pt peaks, $4f_{7/2}$ and $4f_{5/2}$ at 71.2 and 74.3 eV, respectively, suggesting that Pt in the Pt-supported CNTs/carbon paper composite is in the pure metallic state [48]. On the contrary, Pt particles supported on CNTs prepared by the wet impregnation–reduction method contain a mixture of Pt(II) (22%) and Pt(IV) (4%) on the surface [22]. This indicates clearly that the glacial acetic acid has a

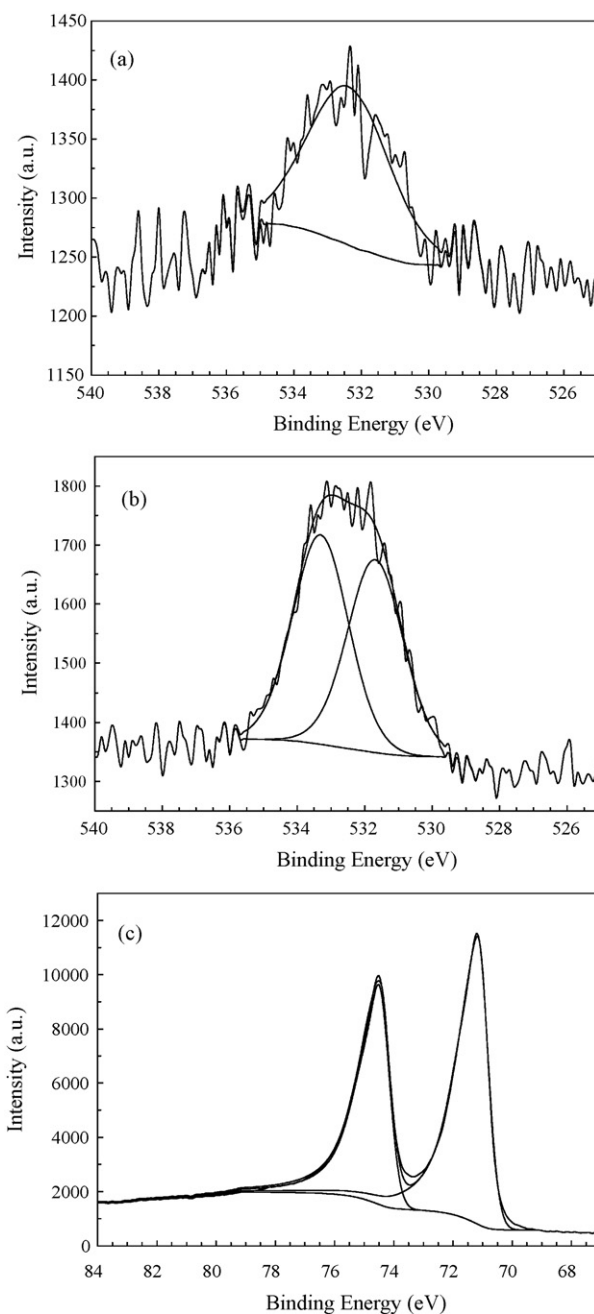


Fig. 4. XPS spectra of the surface of (a) the raw CNTs, (b) glacial acetic acid treated CNTs and (c) Pt nanoparticles deposited on CNTs/carbon paper by reduction with glacial acetic acid.

strong reducing capability, which is also a reason for high-fuel cell performance as shown in Sections 3.2 and 3.3. Recently, a similar acid, formic acid, has been used to reduce Pt on carbon support [46–48] and CNTs [49]. Gonzalez et al. [49–51] reported the preparation of carbon-supported Pt electrocatalysts by reduction with formic acid and showed a higher fuel cell performance when compared to other preparation methods of carbon-supported Pt electrodes [51]. Recently, Tian et al. [52] also used formic acid as a reducing agent for deposition of Pt nanoparticles on CNTs. The CNT-supported Pt catalysts synthesized show significantly higher electrochemically active area

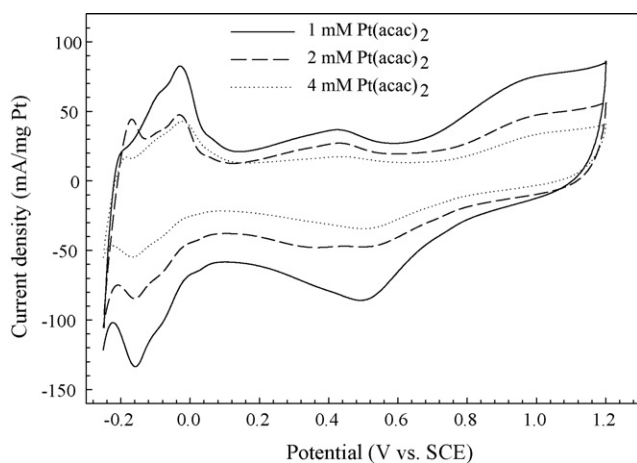


Fig. 5. CVs of Pt/CNT/carbon paper composites prepared from different concentrations of Pt precursor in Ar-saturated 0.5 M H₂SO₄ at scan rate of 50 mV s⁻¹. Current densities normalized with respect to the Pt loading.

and higher catalytic activities toward the methanol oxidation reaction as compared to a commercial E-TEK Pt/C catalyst [52].

3.2. Characterization of Pt/CNT/carbon paper composites by cyclic voltammetry

Electrochemical properties of Pt nanoparticles deposited on CNTs/carbon paper have been investigated by CV. Fig. 5 shows the CVs of Pt/CNT/carbon paper composite electrodes with different Pt loadings in Ar-saturated 0.5 M H₂SO₄ aqueous solution at room temperature. The currents were normalized on the basis of Pt loading. The voltammetric features of all Pt/CNT/carbon paper composite electrodes reveal the typical characteristics of Pt metal [53], with Pt oxide formation in the +0.68 to +1.2 V range, the reduction of Pt oxide at ca. +0.50 V, and the adsorption and deposition of hydrogen between -0.05 and -0.25 V. By using the charge passed for hydrogen adsorption and desorption (Q_H), the Pt areas were calculated electrochemically according to the following formula [22]:

$$A_{EL} = \frac{Q_H}{Q_{ref}(\text{Pt loading})}$$

A_{EL} is expressed in cm² mg⁻¹, where Pt loading is in mg_{Pt} cm⁻² and $Q_{ref} = 0.21$ mC cm⁻². This value corresponds to a surface density of 1.3×10^{15} atom cm⁻², a generally accepted

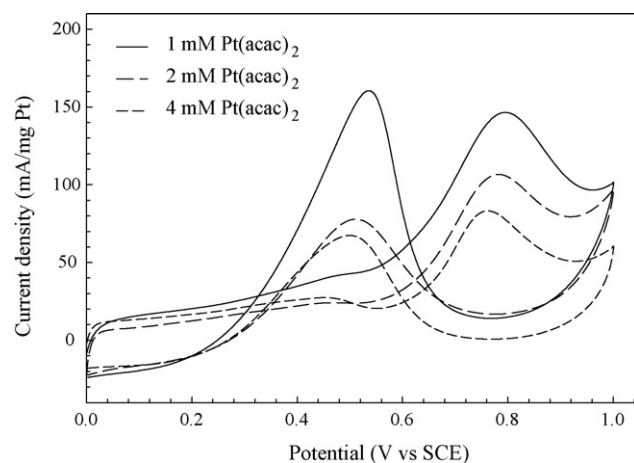


Fig. 6. CVs of Pt/CNT/carbon paper composites prepared from different concentrations of Pt precursor in 2 M MeOH + 1 M H₂SO₄ at scan rate of 50 mV s⁻¹. Current densities normalized with respect to the Pt loading.

value for a polycrystalline Pt electrode [54].

$$A_{EL} (\text{m}^2 \text{g}_{Pt}^{-1}) = 0.1 A_{EL} (\text{cm}^2 \text{mg}_{Pt}^{-1})$$

The calculated values of roughness factors (cm² cm⁻²) as well as roughness factors normalized on the basis of Pt loading are listed in Table 1. The mass-specific surface areas (m² g⁻¹) decrease with increased Pt loading on CNTs. For comparison, the commercial Pt/C electrocatalyst from E-TEK (30 wt.% Pt on carbon black) was also examined with Pt particle size of 2–3 nm at a Pt loading of 0.10 mg cm⁻² and the results are listed in Table 1. In the case of Pt/CNT/carbon paper composite (0.11 mg_{Pt} cm⁻²), the mass-specific surface area is significantly higher as compared to the commercial Pt/C electrode (approximately 61%) (Table 1). This difference is attributed to the unique three-dimensional (3D) structure of the CNTs-based electrode, as we reported previously [44], and well dispersed Pt nanoparticles with sizes of 2–3 nm on the surface of CNTs.

3.3. Electrocatalytic activity of methanol oxidation reaction

Fig. 6 shows the CVs of Pt/CNT/carbon paper composite electrodes with different Pt loadings in Ar-saturated 2 M MeOH and 1 M H₂SO₄ solution at the potential scan rate of 50 mV s⁻¹. The voltammetric features are in good agreement with the literatures [52,55], in which the typical methanol oxidation current peak of a Pt catalyst is at about 0.8 V in the anodic sweep. In

Table 1
Real (active) surface areas and electrochemical characteristics of methanol oxidation on Pt/CNT/carbon paper composite and Pt/C electrodes

Electrode	Pt precursor (mM)	Pt loading ^a (mg cm ⁻²)	S_{EL} ^b (cm ² cm ⁻²)	A_{EL} ^c (m ² g _{Pt} ⁻¹)	Forward peak current density (mA cm ⁻²)	Mass activity (mA mg _{Pt} ⁻¹)
Pt/CNTs	1	0.11	94.6	86.0	16.1	146.4
	2	0.24	187.1	77.9	25.5	106.3
	4	0.42	261.9	62.4	34.7	82.6
30 wt.% Pt/C	–	0.10	33.6	33.6	6.2	62.0

^a Measured by inductively coupled plasma-optical emission spectroscopy.

^b S_{EL} : real surface area obtained electrochemically.

^c A_{EL} : real surface area obtained electrochemically per gram of Pt catalyst.

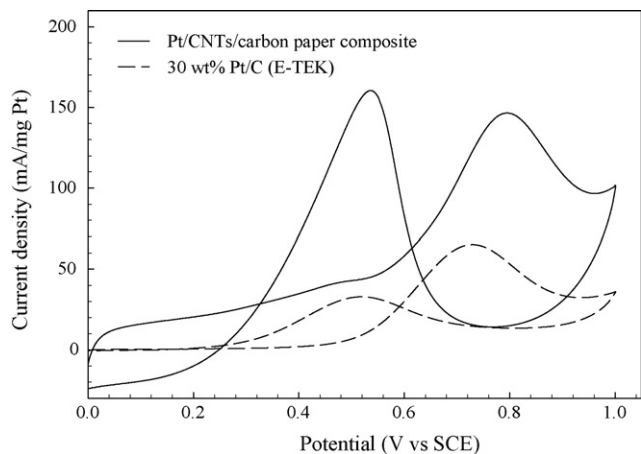


Fig. 7. CVs for methanol oxidation reaction in 2 M MeOH + 1 M H₂SO₄ at Pt/CNT/carbon paper composites with 0.11 mg cm⁻² Pt loading and standard 30 wt.% Pt/C electrode with 0.1 mg cm⁻² Pt loading. Potential scan rate: 50 mV s⁻¹. The current normalized on the basis of Pt loading.

the reverse scan, an oxidation peak is observed around 0.54 V, which is primarily associated with the removal of the absorbed intermediates produced in the forward scan. The mass activity (MA) [56] of the Pt catalyst for methanol oxidation (peak current density of methanol oxidation obtained from CV per unit of Pt loading mass) is calculated and shown in Table 1. It can be obviously observed that the anodic peak current increased with the increase of Pt loadings on CNTs (Table 1).

Fig. 7 compares the CVs for methanol oxidation reaction of a Pt/CNT/carbon paper composite electrode and a commercial Pt/C electrode. The comparison of methanol oxidation reaction with the Pt/CNT/carbon paper composite electrode was made at a Pt loading of 0.11 mg cm⁻². Compared with the commercial Pt/C electrode, the oxidation peak current for the Pt/CNT/carbon paper electrode is about 146.4 mA/mg_{Pt}, which is 57.6% higher than that of the Pt/C electrode (62 mA/mg_{Pt}). This may be attributed to the small size and good dispersion of Pt nanoparticles on the 3D nanotube-based electrodes.

3.4. Single-cell performance

Fig. 8 shows the single-cell performance for the MEA made with Pt/CNT/carbon paper composite electrode (0.42 mg_{Pt} cm⁻²) as cathode and standard E-TEK electrode (0.5 mg_{Pt} cm⁻²) as anode for H₂/O₂. For comparison, the polarization curve of the MEA made with the standard E-TEK electrode (0.5 mg_{Pt} cm⁻²) as anode and cathode is also presented. Polarization characteristics were compared at 80 °C with 25/30 psi g backpressure for the anode and cathode electrodes, respectively (100% humidification condition). It was observed that the Pt/CNT/carbon paper composite showed a better performance than the standard E-TEK electrode especially in the high-current density region. This could be the effect of lower resistance of the CNTs support. It was reported that the CNT-based electrode has improved mass transport [17,23]. At a fixed cell voltage of 0.6 V, the current density of Pt/CNT/carbon paper composite is 1.58 A cm⁻² which is 27% higher than the standard

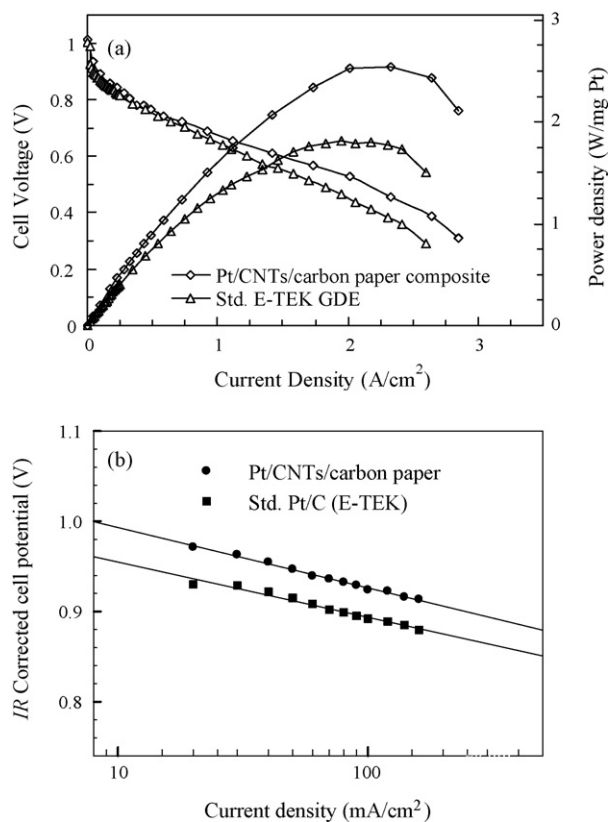


Fig. 8. (a) Polarization characteristics of the MEAs fabricated with CNTs electrode (0.42 mg_{Pt} cm⁻²) and standard E-TEK electrode (LT140E-W; 0.5 mg_{Pt} cm⁻²) as cathode electrodes for H₂/O₂ at 80 °C, Nafion 112 membrane, 25/30 psi g anode and cathode back pressure. Anode electrodes were E-TEK electrode with 0.5 mg_{Pt} cm⁻². (b) IR corrected Tafel plots for comparison of kinetic parameters (Table 2).

E-TEK electrode (1.16 A cm⁻²). The corresponding power densities normalized on the basis of Pt loading were 2.19 W mg_{Pt}⁻¹ (Pt/CNT/carbon paper composite) and 1.42 W mg_{Pt}⁻¹ (standard E-TEK electrode) at 0.6 V, showing a significant increase in power density of about 0.77 W mg_{Pt}⁻¹ for the Pt/CNT/carbon paper composite.

To obtain detailed information about the electrode kinetic parameters of oxygen reduction, the experimental cell potential (*E*) and current density (*i*) data was analyzed using the following equation [57]:

$$E = E^0 - b \log i - Ri \quad (1)$$

where

$$E^0 = E_r + b \log i^0 \quad (2)$$

In these equations, *E_r* is the reversible potential for the oxygen electrode reaction, *b* is the Tafel slope, *i*₀ is the exchange current density for the oxygen reduction, and *R* is the predominantly the ohmic resistance in the electrode and electrolyte responsible for the linear variation of potential vs. current density plot. The experimental data was fitted to the above equation by a non-linear least-square method in order to evaluate the kinetic parameters from regression analysis. The resulting values are given in Table 2. The Tafel slope of Pt/CNTs/carbon

Table 2

PEMFC Tafel kinetic parameters for oxygen reduction obtained from Pt/CNT/carbon paper composite electrode with Pt loading of $0.42 \text{ mg}_{\text{Pt}} \text{ cm}^{-2}$

Electrode	E_0 (mV)	b (mV decade $^{-1}$)	$I_{900 \text{ mV}}$ (mA cm^{-2})	$I_{900 \text{ mV}}$ ($\text{mA mg}_{\text{Pt}}^{-1}$)
Pt/CNTs/carbon paper	1059	66.3	248.1	590.7
Std. Pt/C (E-TEK)	1016	60.2	84.4	168.7

Values from a representative standard Pt/C commercial (E-TEK) electrode ($0.5 \text{ mg}_{\text{Pt}} \text{ cm}^{-2}$) are shown.

paper composite and commercial E-TEK electrodes is found to be ca. 0.06 V which is common to most supported and unsupported Pt electrodes [58]. It is clearly evident that the current density at 900 mV ($i_{900 \text{ mV}}$) for Pt/CNT/carbon paper composite is significantly higher as compared to the E-TEK electrode (approximately 66%) (Table 2). This difference is attributed to the higher dispersion of Pt nanoparticles on the surface of CNTs as well as the unique 3D structure of the CNT-based electrode [17,22,44,59].

4. Conclusions

A novel synthetic method has been successfully developed to deposit Pt nanoparticles on CNTs grown on commercially used carbon paper by reduction of Pt precursor with glacial acetic acid. This method allows us to deposit high-loading Pt nanoparticles monodispersed on CNTs. XPS analysis showed that glacial acetic acid plays a critical role in producing surface functional groups on the CNTs. The monodispersed Pt particles on the surface of CNTs have been found to be $2\text{--}4 \text{ nm}$ in size depending on Pt precursor concentrations. The resultant Pt/CNT/carbon paper composite electrode shows higher performance in comparison to standard E-TEK electrode, which can be attributed to the improved dispersion of Pt nanoparticles on the CNTs surface and to the 3D structure of CNT-based electrodes.

Acknowledgements

This research was supported by Natural Sciences and Engineering Research Council of Canada (NSERC), INCO, Ontario Research Fund (ORF), Materials and Manufacturing Ontario (MMO), Canada Foundation for Innovation (CFI), Canada Research Chair (CRC) Program, Ontario Early Researcher Award (ERA) and the University of Western Ontario.

References

- [1] K. Kordesch, G. Simander, Fuel Cells and their Applications, VCH, Germany, 1996, p. 73.
- [2] L.J.M. Blomen, M.N. Mugerwa, Fuel Cell Systems, Plenum Press, New York, 1993.
- [3] K. Kinoshita, J. Electrochem. Soc. 137 (1990) 845–848.
- [4] W.X. Chen, J.Y. Lee, Z. Liu, Chem. Commun. (2002) 2588–2589.
- [5] T.R. Ralph, M.P. Hogarth, Platinum Met. Rev. 46 (2002) 3–14.
- [6] D.A. Stevens, M.T. Hicks, G.M. Haugen, J.R. Dahn, J. Electrochem. Soc. 152 (2005) A2309–A2315.
- [7] A. Wieckowski, E.R. Savinova, C.G. Vayenas, Catalysis and Electrocatalysis at Nanoparticle Surface, Marcel Dekker, New York, 2003.
- [8] J.G. Liu, Z.H. Zhou, X.X. Zhao, Q. Xin, G.Q. Sun, B.L. Yi, Phys. Chem. Chem. Phys. 6 (2004) 134–137.
- [9] Y. Shao, G. Yin, Y. Gao, J. Power Sources 171 (2007) 558–566.
- [10] Y. Shao, G. Yin, J. Zhang, Y. Gao, Electrochim. Acta 51 (2006) 5853–5857.

- [11] R. Borup, J. Meyers, B. Pivovar, Y.S. Kim, R. Mukundan, N. Garland, D. Myers, M. Wilson, F. Garzon, D. Wood, P. Zelenay, K. More, K. Stroh, T. Zawodzinski, X.J. Boncella, J.E. McGrath, O.M. Inaba, K. Miyatake, M. Hori, K. Ota, Z. Ogumi, S. Miyata, A. Nishikata, Z. Siroma, Y. Uchimoto, K. Yasuda, K.-I. Kimijima, N. Iwashita, Chem. Rev. 107 (2007) 1–48.
- [12] P.M. Ajayan, O.Z. Zhou, Topics Appl. Phys. 80 (2001) 391–425.
- [13] C. Pham-Huu, N. Keller, V.V. Roddatis, G. Mestl, R. Schloegl, M.J. Ledoux, Phys. Chem. Chem. Phys. 4 (2002) 514–521.
- [14] R.H. Baughman, A.A. Zakhidov, W.A. Heer, Science 297 (2002) 787–793.
- [15] Z. Liu, X. Lin, J.Y. Lee, W. Zhang, M. Han, L.M. Gan, Langmuir 18 (2002) 4054–4060.
- [16] M. Carmo, V.A. Paganin, J.M. Rosolen, E.R. Gonzalez, J. Power Sources 142 (2005) 169–176.
- [17] X. Wang, M. Waje, Y. Yan, Electrochem. Solid-State Lett. 8 (2005) A42–A44.
- [18] N. Rajalakshmi, H. Ryu, M.M. Shaijumon, S. Ramaprabhu, J. Power Sources 140 (2005) 250–257.
- [19] G. Girishkumar, K. Vinodgopal, P.V. Kamat, J. Phys. Chem. B 108 (2004) 19960–19966.
- [20] E.S. Steigerwalt, G.A. Deluga, C.M. Lukehart, J. Phys. Chem. B 106 (2002) 760–766.
- [21] T. Matsumoto, T. Komatsu, H. Nakano, K. Arai, Y. Nagashima, E. Yooa, T. Yamazaki, M. Kijima, H. Shimizu, Y. Takasawa, J. Nakamura, Catal. Today 90 (2004) 277–281.
- [22] D. Villers, S.H. Sun, A.M. Serventi, J.P. Dodelet, J. Phys. Chem. B 110 (2006) 25916–25925.
- [23] W. Li, C. Liang, W. Zhou, J. Qiu, Z. Zhou, G. Sun, Q. Xin, J. Phys. Chem. B 107 (2003) 6292–6299.
- [24] G. Wu, Y.S. Chen, B.Q. Xu, Electrochem. Commun. 7 (2005) 1237–1243.
- [25] G. Che, B.B. Lakshmi, C.R. Martin, E.R. Fisher, Langmuir 15 (1999) 750–758.
- [26] Z. He, J. Chen, D. Liu, H. Zhou, Y. Kuang, Diamond Relat. Mater. 13 (2004) 1764–1770.
- [27] Y. Shao, G. Yin, Y. Gao, P. Shi, J. Electrochem. Soc. 153 (2006) A1093–A1097.
- [28] X. Wang, W. Li, Z. Chena, M. Waje, Y. Yan, J. Power Sources 158 (2006) 154–159.
- [29] K. Lee, J. Zhang, H. Wang, D.P. Wilkinson, J. Appl. Electrochem. 36 (2006) 507–522.
- [30] L.M. Ang, T.S.A. Hor, G.Q. Xu, C.H. Tung, S.P. Zhao, J.L.S. Wang, Chem. Mater. 11 (1999) 2115–2118.
- [31] Y.C. Xing, J. Phys. Chem. B 108 (2004) 19255–19259.
- [32] D.-J. Guo, H.-L. Li, Electroanalysis 17 (2005) 869–872.
- [33] Z. He, J. Chen, D. Liu, H. Tang, W. Deng, Y. Kuang, Mater. Chem. Phys. 85 (2004) 396–401.
- [34] B.C. Satishkumar, E.M. Vogl, A. Govindaraj, C.N.R. Rao, J. Phys. D: Appl. Phys. 29 (1996) 3173–3176.
- [35] Z.Y. Sun, Z.M. Liu, B.X. Han, Y. Wang, J.M. Du, Z.L. Xie, G.J. Han, Adv. Mater. (Weinheim, Germany) 17 (2005) 928–932.
- [36] R. Yu, L. Chen, Q. Liu, J. Lin, K.-L. Tan, S.C. Ng, H.S.O. Chan, G.-Q. Xu, T.S.A. Hor, Chem. Mater. 10 (1998) 718–722.
- [37] Q. Xu, L. Zhang, J. Zhu, J. Phys. Chem. B 107 (2003) 8294–8296.
- [38] S. Arai, M. Endo, N. Kaneko, Carbon 42 (2004) 641–644.
- [39] S.D. Thompson, L.R. Jordan, M. Forsyth, Electrochim. Acta 46 (2001) 1657–1663.
- [40] D.-J. Guo, H.-L. Li, J. Electroanal. Chem. 573 (2004) 197–202.
- [41] C.C. Chen, C.F. Chen, C.H. Hsu, I.H. Li, Diamond Relat. Mater. 14 (2005) 770–773.

- [42] C.-L. Sun, L.-C. Chen, M.-C. Su, L.-S. Hong, O. Chyan, C.-Y. Hsu, K.-H. Chen, T.-F. Chang, L. Chang, *Chem. Mater.* 17 (2005) 3749–3753.
- [43] J. Wang, G. Yin, Y. Shao, Z. Wang, Y. Gao, *J. Electrochem. Soc.* 154 (2007) B687–B693.
- [44] X. Sun, R. Li, D. Villers, J.P. Dodelet, S. Desilets, *Chem. Phys. Lett.* 379 (2003) 99–104.
- [45] S.L. Gojkovic, S.K. Zecevic, R.F. Savinell, *J. Electrochem. Soc.* 145 (1998) 3713–3720.
- [46] A.M. Kannan, V.P. Veedu, L. Munukutla, M.N. Ghasemi-Nejhad, *Electrochem. Solid-State Lett.* 10 (2007) B47–B50.
- [47] U. Zielke, K.J. Hutter, W.P. Hoffman, *Carbon* 34 (1996) 983–998.
- [48] C.-L. Lee, Y.-C. Ju, P.-T. Chou, Y.-C. Huang, L.-C. Kuo, J.-C. Oung, *Electrochem. Commun.* 7 (2005) 453–458.
- [49] E.R. Gonzalez, E.A. Ticianelli, A.I.N. Pinheiro, J. Perez, *Brazilian Patent, INPI-SP No. 00321*, (1997).
- [50] J.R.C. Salgado, E. Antolini, E.R. Gonzalez, *J. Power Sources* 141 (2005) 13–18.
- [51] J.R.C. Salgado, E.R. Gonzalez, *Eclat. Quim.* 28 (2003) 77–81.
- [52] Z.Q. Tian, S.P. Jiang, Y.M. Liang, P.K. Shen, *J. Phys. Chem. B* 110 (2006) 5343–5350.
- [53] A.J. Bard, L.R. Faulkner, *Electrochemical Methods, Fundamentals and Applications*, Wiley, New York, 1980.
- [54] A. Pozio, M.D. Francesco, A. Cemmi, F. Cardellini, L. Giorgi, *J. Power Sources* 105 (2002) 13–19.
- [55] Y. Lin, X. Cui, C. Yen, C.M. Wai, *J. Phys. Chem. B* 109 (2005) 14410–14415.
- [56] F. Gloaguen, J.-M. Leger, C. Lamy, *J. Appl. Electrochem.* 27 (1997) 1052–1060.
- [57] E.A. Ticianelli, C.R. Derouin, A. Redondo, S. Srinivasan, *J. Electrochem. Soc.* 135 (1988) 2209–2214.
- [58] A. Parthasarathy, S. Srinivasan, A.J. Appleby, C.R. Martin, *J. Electroanal. Chem.* 339 (1992) 101–121.
- [59] C. Wang, M. Waje, X. Wang, J.M. Tang, R.C. Haddon, Y. Yan, *Nano Lett.* 4 (2004) 345–348.